PNC TN941 81—18

Experiments on Local Core Anomaly Detection by Fluctuations of Temperature and Flow Rate at LMFBR Fuel Subassembly Outlets

February, 1981

Power Reactor and Nuclear Fuel Development Corporation

Mitsubishi Electric Corporation

PNC TN941 81—18

February, 1981

Experiments on Local Core Anomaly Detection by Fluctuations of Temperature and Flow Rate at LMFBR Fuel Subassembly Outlets

K. Haga*, T. Ogino** and H. Inujima**

Abstract

Several series of out-of pile safety experiments have been conducted using heater pin bundles. Sodium boiling, fission product (FP) gas release and local flow blockage phenomena were measured in the test sections of a sodium loop named SIENA at the Oarai Engineering Center, PNC.

In almost all test sections an eddy durrent flow-meter and Chromel-Alumel thermocouples were installed at the outlet of the bundle for the convenience of monitoring. The alternating current components of the recorded signals were examined from the view point of local core anomaly detection.

The simulated LMFBR fuel subassemblies were 37-pin or 61-pin bundle geometries, in which 6.5 mm diameter pins were heated for the axial length of around 450 mm. A 5 mm thick stainless steel plate was inserted in the heated region to form a blockage. The root mean square (RMS) value, and power spectral density (PSD) of the temperature and flow fluctuations, and the transfer function and coherence between temperature fluctuations were examined. The studies showed that the temperature fluctuation transferred the information on local boiling toward the end of the bundle, but hardly to the outlet. The temperature fluctuation at the outlet may be generated mainly by the turbulent mixing of the coolant flowing through the passage from the end of the bundle to the measured position. Consequently, it can be considered that the local boiling may be detected only

---

Present work was made in the cooperative study between PNC and Mitsubishi Electric Corp. under agreement 550F001.

* Fast Reactor Safety Section, Oarai Engineering Center, PNC.

** Central Research Laboratory, Mitsubishi Electric Corporation,

when the local boiling region is large enough to affect the temperature distribution at the outlet of the bundle or generate global flow oscillations due to void formation and collapse. The burst type one-pin failure can be detected by the flow fluctuation.

INTRODUCTION

For the safe operation of a liquid metal fast breeder reactor (LMFBR), it is important to detect any local fault in its initial stage. Some types of anomaly detection systems are being considered for use in the MONJU plant. One of them is to use flowmeters and thermocouples at the exit of core subassemblies. This method has an advantage that the sensors serve to get information of core normal operating conditions (temperature profile across the core and flow rate of each subassembly). If only the DC components of flow and temperature are used, they will be useful for anomaly detection when a subassembly is locally blocked by more than 60% of the total flow area, because the flow reduces by more than 10% of its normal value[1]. On the other hand the use of their AC components is more promising to supply information for anomaly detection in its early stage. Many efforts have been concentrated in this area[2],[3],[4],[5].

Several series of out-of-pile local fault experiments have been conducted in the Fast Reactor Safety Section, Oarai Engineering Center, PNC. The temperature increases due to blockages and FP gas release were measured. Local boiling phenomena were also observed in this series of experiments, in which electrically heated pin bundles were used. At the outlet of the test section an eddy current flowmeter and thermocouples were assembled. The signals from the sensors, mainly the fluctuations, were analyzed from the view point of anomaly detection.

The present paper presents the experimental procedure and the application of an anomaly detection method to the obtained data. Discussions on the feasibility of local core anomaly detection by use of the temperature and flow fluctuations are also given. The contents of the present paper are mainly the summaries of the authors' two previous papers[6],[7]. In addition to the summaries a future plan on this study is introduced.

EXPERIMENTAL EQUIPMENT AND OPERATING PROCEDURE

The experiments were carried out in the Sodium Boiling and Fuel Failure Propagation Test Loop. Figure 1 shows the schematic representation of one of the local blockage test sections. The hexcan contains an electrically heated 61-pin bundle. The diameter of each pin is 6.5 mm and the pin pitch is 7.9 mm. The clearance of neighboring pins is kept constant by wire spacers. The outer 24 pins of the test section are dummy pins. The 36% central-type tight blockage is attached at the middle position of the heated section. The power distribution is uniform along the heated length of 450 mm.

Chromel-Alumel thermocouples represented by T-XXXX in Fig. 1 are located at various positions of the test section. The thermocouple T-004 is an ungrounded type sheathed thermocouple whose diameter is 4.8 mm, and the others are grounded type sheathed thermocouples whose diameters are 0.3 mm. An eddy current type flowmeter is installed at the outlet of the bundle.

The data acquisition system of the fluctuation signals is shown in Fig. 2. The temperature and flow signals are transmitted to a control room using double shielded cables. The fluctuation signals are obtained from specially designed fluctuation measuring circuits. The circuits consist of a low noise AC amplifier and a band pass filter. The specifications of these components are as follows:

AC amplifier	gain	: 60 dB (max.)
	low cut off frequency	: 0.01 Hz
Band pass filter	low cut off frequency	: 0.01 Hz
	slope	: 40 dB/dec
	high cut off frequency	: 15 Hz
	slope	: 200 dB/dec

Table 1 is a list of test sections used in the present studies.

Operating procedure

(1) Single phase flow experiments

In order to study the statistical properties of the fluctuation signals, many liquid flow experiments were carried out in the test sections with and without blockage.

(2) Local boiling experiments

These experiments were performed in the test section with blockage. The flow rate was set and heater pins were adjusted to a fixed power level. When a steady state condition was reached, the power level of the heater pins was gradually increased. Inception of boiling was monitored by the pressure signal at the outlet of the bundle.

(3) Gas release experiments

In order to evaluate the sensitivity of the eddy current type flow meter to gas in the coolant, steady state gas release experiments were carried out at various gas to liquid flow ratios in a test section without blockage.

STATISTICAL PROPERTIES OF TEMPERATURE AND FLOW FLUCTUATIONS

The RMS value of the temperature fluctuation at the outlet of the 37F Test Section is plotted against heat flux and against flow rate in Fig. 3(a) and Fig. 3(b), respectively. It is shown that the RMS of the temperature fluctuation increases linearly with heat flux for fixed flow rate. The RMS of the flow fluctuation is plotted against flow rate in Fig. 3(c) with the parameter of exciting frequency of the eddy current type flowmeter. The ratio of the RMS of the flow fluctuation to the flow rate increases with exciting frequency.

The power spectral densities (PSDs) of the temperature and the flow fluctuations are shown in Fig. 4(a) and Fig. 4(b). Both of these hardly attenuate in the frequency range from 0 to 10 Hz. Above 10 Hz frequency, characteristics of the fluctuation measuring circuits strongly affect the values of the PSDs.

Auto-regressive models (AR-models) are fitted to the temperature and the flow fluctuations. Validity of representing the fluctuations by AR-models can be shown by the test of the residual random process for whiteness. Typical results of the test are given in Fig. 5(a) and Fig. 5(b). These figures show that the fluctuations can be represented by AR-models, since the residual random processes can be regarded as white in the frequency range from 0 to 30 Hz.

ANOMALY DETECTION METHOD

An anomaly detection method which uses a fluctuation signal is generally based on the comparison of a typical statistical index of the fluctuation signals at the normal state with that at an anomalous state. PSDs, RMS values, Skewness factors, etc. are usually used for this purpose. It is desirable that the anomaly detection method takes into account enough information from fluctuation signals to judge the operational status of a reactor.

Since the temperature and the flow fluctuations can be expressed in AR-models, as is shown in the previous section, an anomaly detection method which uses the AR-model was developed. The method is called a whiteness test method (WTM) in this paper.

Let Xi (i = 1,2, ... , N) be a time series of the fluctuation signal. Then AR-model of Xi is given by Eq. (1).

$$X_n = \sum_{j=1}^{M} \hat{a}j\, X_{n-j} + \varepsilon_n \qquad (1)$$

where

ε_n : prediction error of X_n (residual random process)

$\hat{a}j$: AR-model coefficients (j = 1,2, ... , M)

$\hat{a}j$ (j = 1,2, ... , M) are obtained by the least squares method, and M is determined so as to minimize FPE (final prediction error) defined by Eq. (2)[8].

$$FPE = \frac{N+M+1}{N-M-1} \left\{ \frac{1}{N-M} \sum_{j=M+1}^{N} \varepsilon_j^2 \right\} \qquad (2)$$

The whiteness test method is processed in the following steps.

Step 1. $\varepsilon_n = \underline{Xn} - \sum_{i=1}^{M} \hat{a}i\, \underline{Xn-i}$

ε_n : residual random process of fluctuation of $\underline{Xn}$

$\underline{Xn}$: fluctuation to be diagnosed

The AR-model is determined by use of the data at the normal operating state.

Step 2. $\psi\varepsilon\varepsilon(n, \tau) = \frac{1}{\ell} \sum_{j=1}^{N_0} \varepsilon_{n+j} * \varepsilon_{n+j-\tau} \qquad \tau = 1, 2, \ldots, \tau max$

where ℓ : number of data used for computing $\phi\varepsilon\varepsilon(n+N_0,\tau)$

N_0 : number of sampled data in the monitoring interval

τmax : maximum lag number of the autocovariance function $\phi\varepsilon\varepsilon(n,\tau)$

Step 3. $\phi\varepsilon\varepsilon(n+N_0,\tau) = \phi\varepsilon\varepsilon(n,\tau) + \Delta\phi\varepsilon\varepsilon(n,\tau)$

$= \phi\varepsilon\varepsilon(n,\tau) + \psi\varepsilon\varepsilon(n,\tau) - \psi\varepsilon\varepsilon(n-\ell,\tau)$

The values of ℓ and N_0 are so selected that ℓ/N_0 shall be an integer.

Step 4. $$I(n+N_0,M,L,\tau max) = \sum_{\tau=1}^{\tau max} \left|\phi\varepsilon\varepsilon(n+N_0,\tau)\right|^2 \quad (3)$$

$I(n+N_0,M,L,\tau max)$: anomaly detection index of the WTM (AR-index)

Step 5. $I^{\ell}_{\ell mt} \leq I(n+N_0,M,L,\tau max) \leq I^{u}_{\ell mt}$; Normal

Otherwise : Anomaly

where $I^{\ell}_{\ell mt}$ and $I^{u}_{\ell}mt$ are lower and upper alarm levels.

This WTM algorithm has been developed for a mini-computer system. The values of L, M, N_0 and τmax used in the experimental data analysis were 120∿240, 3, 30∿50, and 6∿10, respectively.

APPLICATION OF DATA PROCESSING METHODS ON TEMPERATURE AND FLOW FLUCTUATIONS UNDER LOCAL BOILING CONDITIONS

To illustrate the application of the data processing method on experiments, one typical run of local boiling in a 61-pin bundle was chosen as an example.

Figure 6 shows the signals obtained in the Run No. 61WLB-101. FEC-1A is the flow fluctuation signal measured by the eddy current type flowmeter. T-024 and T-024A are the temperature and its fluctuation signals measured at the outlet, respectively. T-021G and T-021GA are the temperature and fluctuation readings of the thermocouple whose location is 34 mm downstream of the blockage. P-111 is the pressure at the outlet. Inception of local boiling was monitored by this pressure signal. F-103 is the flow signal at the inlet of the test section.

The inlet sodium flow was decreased stepwise at 62, 86, 157 and 251 sec. The local boiling was initiated at about 95 sec, after the second reduction of flow rate. Three steady state local boiling tests were conducted under different conditions: "Local boiling I", "Local boiling II" and "Local boiling III". At the second and third reductions of flow rate, conspicuous increases were found in both the temperature and its fluctuation signals measured at the position immediately behind the blockage (T-021G and T-021GA). During the local boiling II and III tests, T-021G had reached the sodium saturation temperature, on the other hand, the temperature at the outlet, T-024, increased gradually by only 3 to 5°C at each step of flow reduction. Conspicious changes were hardly found in the outlet temperature fluctuation, T-024A, during all the flow decreases except the second one. The flow fluctuation, FEC-1A, did not show any visible changes not only during the flow reductions but also at the onset of local boiling.

RMS Value of Temperature Fluctuation

Figure 7 shows the RMS values of temperature fluctuations observed at several axial positions behind the blockage. The following items were made clear from these analyses:

(1) At the position immediately behind the blockage, the RMS values of temperature fluctuations under local boiling conditions were about 15 times larger than that under non-boiling condition.

(2) In the downstream beyond 144 mm from the blockage, noticeable changes were not found in the RMS values of temperature fluctuations between the two conditions.

(3) The RMS values of temperature fluctuations observed at the outlet were in all cases about 5 times larger than those at the end of the bundle.

PSD of Temperature Fluctuation

Figures 8 and 9 show the PSDs of the same temperature fluctuations under non-boiling and local boiling III conditions. The temperature fluctuations in the bundle with boiling had spectral peaks around 4 Hz. The peaks were due to the repetitive cycle of bubble formation and collapse. On the other hand, the temperature fluctuation at the outlet had no spectral peak.

PSD of Flow Fluctuation

As shown in Fig. 10, no conspicuous feature of local boiling was found in the PSDs of flow fluctuations measured at the outlet of the bundle.

Transfer and Coherence Functions of Temperature Fluctuations

Figures 11 and 12 show the transfer and coherence functions between several couples of temperature fluctuations under the local boiling III condition: one is always fixed to that measured immediately behind the blockage (T-021GA) and another is selected from those measured at various downstream locations.

Concerning the transfer functions, peaks appeared around 4 Hz only for the cases with the temperature fluctuations measured within the region less than 66 mm (T-021J) downstream of the blockage. Otherwise, the peak was attenuated remarkably. In the case of coherence functions, conspicuous peaks were found within the whole bundle section. However, it was hardly found at the outlet.

These analyses made clear the following items:

(1) The inconsistency between transfer and coherence functions, both calculated with the temperature fluctuation at the end of the bundle, was mainly due to the strong attenuation of fluctuation level during the axial motion of fluid (see Fig. 7). This fact proves that the information on local boiling is transferred almost linearly to the end of the bundle even though it is fairly small. Figure 7 shows the amount of information on local boiling transferred to the end of the bundle.

(2) At the outlet of the bundle, both transfer and coherence functions are small in the whole frequency range. From this fact, it is deduced that the temperature fluctuation at the outlet is hardly correlated to that at the boiling position. The temperature fluctuation at the outlet may be generated mainly by the turbulent mixing of the coolant flowing through the passage from the end of the bundle to the measured position, since the RMS value of temperature fluctuation at the outlet is about 5 times larger than that at the end of the bundle.

FEASIBILITY OF LOCAL BOILING DETECTION

Figures 13 and 14 show the result of the anomaly detection by the RMS method and the WTM applied to the temperature and flow fluctuations, where the sampling interval and averaging time were selected to be 0.016 and 8.0 seconds, respectively. Concerning the RMS values of temperature and flow fluctuations, noticeable changes were not found during the run. In the AR index of temperature fluctuations, remarkable increases were found immediately after the reductions of flow rate. However, conspicuous increases were not always found in the AR index of flow fluctuations.

The RMS values of temperature and flow fluctuations under local boiling conditions were larger than those under non-boiling conditions. The amount of the difference ($\leq 20\%$) was, however, insufficient to detect local boiling.

Figure 15 shows the ratio of the average AR index under steady state local boiling conditions to that under non-boiling conditions (averaging time is 32 sec). The ratio of the temperature fluctuations was from 1.5 to 1.8, and that of the flow fluctuations was from 2.0 to 2.5. This figure also shows that the ratio increases with boiling intensity.

As mentioned in the previous section, there was little correlation between temperature fluctuations at the boiling position and those (or the flow fluctuations) at the outlet of the bundle. Consequently, it is easy to infer that the local boiling may be detected only when the local boiling region is large enough to affect the temperature distribution at the outlet of the bundle or generate global flow oscillations due to void formation and collapse.

There is an another problem in detecting an anomaly by thermocouples. The signals showed in Fig. 6 to Fig. 15 were measured by thermocouples which had time constants around 0.01 sec. However in a typical reactor plant system, with each thermocouple in a protective well, the time constant of the core-outlet thermocouple is very large. Even if helium gas is charged inside the well, the time constant may be more than 2.0∿3.0 sec.

Figures 16(a)∿16(d) show the effect of the thermocouple time constant on the measured temperature fluctuation. Local boiling initiated at 40 sec. The original data were measured by a thermocouple whose time constant was 0.53 sec. The other data were artificially obtained by a low-pass processing operation. It can be seen from these figures that as the time constant increases, the temperature fluctuations decrease.

For the reasons mentioned above it may be very difficult to use the temperature fluctuation signal of thermocouples for anomaly detection in a reactor system.

DETECTION OF PIN FAILURE BY FLOW FLUCTUATION

An eddy-current type flow meter can be used for not only flow measurement but also gas detection in the coolant. The RMS of the flow fluctuation is plotted in Fig. 17 against gas volumetric flow ratio with the parameter of exciting frequency. The figure shows that the sensitivity to gas gets higher with the increase of the exciting frequency. The exciting frequency is usually selected to be 200～500 Hz, so the RMS of the flow fluctuation at the 0.5% gas volumetric flow ratio is at least six times bigger than that without gas. Figure 18 shows the scale of a detectable one-pin failure under the MONJU operating conditions, which has been obtained from the above experimental data and through the analysis of fission gas release rate by a critical flow model. The figure shows that the burst-type one-pin failure in some conditions can be detected by the flow fluctuation. The typical examples of detectable one-pin failure conditions are as follows.

Initial gas plenum pressure	Equivalent pin hole diameter
$10 * 10^5$ N/m^2	0.9 mm
$50 * 50^5$ N/m^2	0.3 mm

SUMMARY

The statistical properties of the temperature and flow fluctuations have been studied in the several series of out-of-pile local fault experiments. The results are summarized below.

(1) The temperature fluctuations caused by a local blockage can hardly transfer to the end of pin bundle. To detect local blockage by temperature fluctuations it will be necessary that the blocked flow area is so large as to decrease the inlet flow rate causing the temperature profile change or conspicuous increase of temperature level at the outlet of a subassembly.

(2) A strong correlation was found for the temperature fluctuations observed at the boiling position and at the end of the bundle, while the correlation has not been clarified with regard to the fluctuations at the subchannel outlet.

(3) It may be passible to detect a local boiling accident when the boiling intensity becomes fairly large.

(4) The burst-type one-pin failure can be detected by the flow fluctuation (under certain conditions).

(5) The whiteness test method (WTM) of analyzing a fluctuation signal was a sensitive and reliable method for detecting a local accident within a subassembly.

As is indicated in the conclusion (3), when the boiling intensity becomes fairly large, local boiling may be detected by fluctuations at the outlet of subassembly. Hence it is important to identify the limit of scale of boiling which is recognized by the outlet temperature or flowrate. To make this evaluation, a larger bundle test section is expected to supply useful informations.

Figure 19 shows the last and largest test section in this series of experiments. The 91-pin bundle local blockage experiments start at the beginning of 1981 and will continue all through the year.

REFERENCES

[1] F. Nakamura and K. Miyaguchi et al., "HYDRAULIC SIMULATION OF LOCAL BLOCKAGE IN LMFBR FUEL SUBASSEMBLY," 8th Liquid Metal Boiling Working Group Meeting, Mol (1978).

[2] D.N. Fry and W.H. Leavell, "TEMPERATURE NOISE ANALYSIS AT THE EXIT OF BLOCKED AND UNBLOCKED 19-PIN ELECTRICALLY HEATED LMFBR FUEL SUB-ASSEMBLY MOCKUPS," ORNL-TM-5464, Oak Ridge National Laboratory, (Aug. 1976).

[3] E. Ohlmer and D. Schwalm, "THE USE OF THE AMPLITUDE DISTRIBUTION FUNCTION IN A SIMULATED REACTOR SUBASSEMBLY," Atomkernenergie, 25, 281 (1975).

[4] E.J. Burton, P.G. Bentley et al., "AN OVER VIEW OF THE DEVELOPMENT OF DIAGNOSTIC TECHNOQUES FOR FAST REACTOR," International Meeting of Fast Reactor Safety Technology (1979).

[5] D. Smith et al., "DFR SPECIAL EXPERIMENTS," International Symposium on Design, Construction and Operating Experiment of Demonstration LMFBR, International Atomic Energy Agency, Vologna (1978).

[6] T. Ogino, H. Inujima et al., "FEASIBILITY STUDY OF LOCAL CORE ANOMALY DETECTION BY USE OF TEMPERATURE AND FLOW FLUCTUATIONS AT LMFBR FUEL SUBASSEMBLY OUTLET," International Meeting on Fast Reactor Safety Technology, Seattle (1979).

[7] H. Inujima, T. Ogino et al., "TEMPERATURE AND FLOW FLUCTUATIONS UNDER LOCAL BOILING IN A SIMULATED FUEL SUBASSEMBLY," 9th Liquid Metal Boiling Working Group Meeting, Casaccia (1980).

[8] H. Akaike, "FITTING AUTOREGRESSIVE MODELS FOR PREDICTION," Ann. Institute of Statistical Mathematics, 21, pp.243∿247, (1979).

Table 1　Geometries of test sections

Name of Test Section	Bundle Size (pins)	Blockage		Spacer
19A	19	No		Wire
37B	37	Central	27%	Grid
37C	37	Edge	50%	Grid
37D	37	Central	26%	Wire
37E	37	Edge	50%	Wire
37F	37	No		Wire
61A	61	Central	36%	Wire

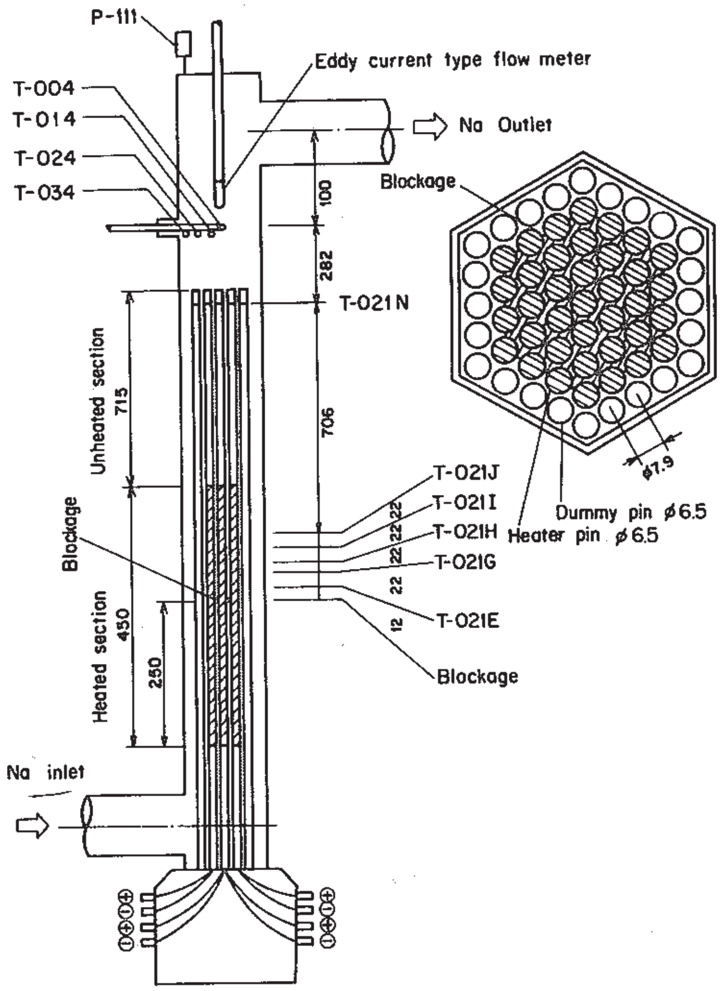

Fig. 1 Locally blocked 61-pin bundle test section

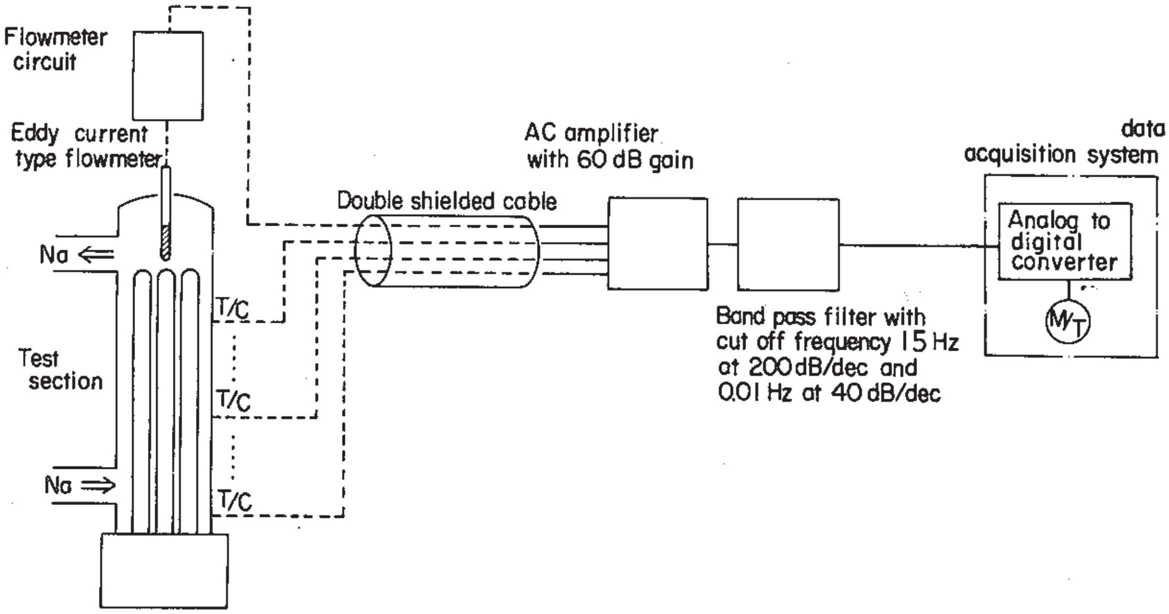

Fig. 2 Schematic diagram of the data acquisition system of fluctuation signals

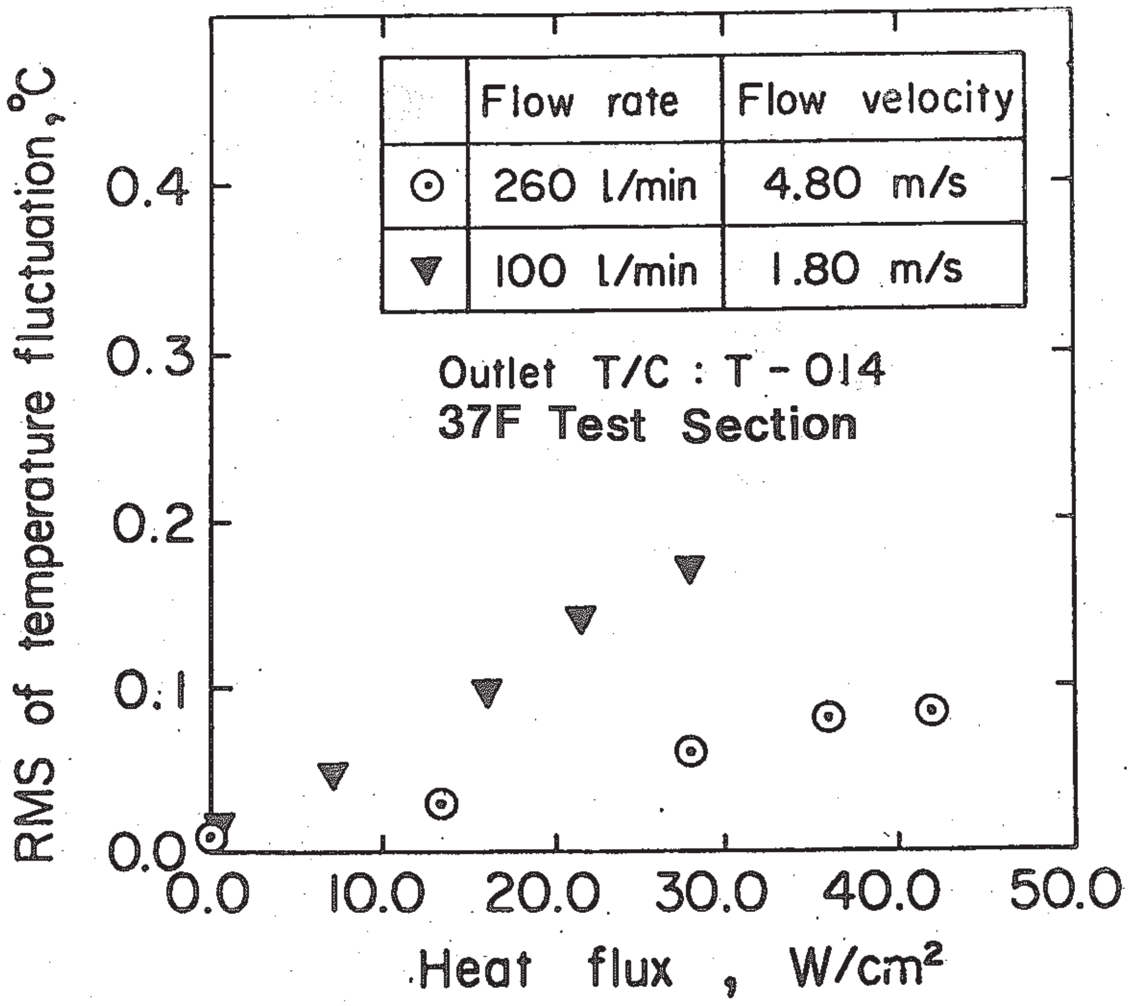

Fig. 3(a) Effect of heat flux on RMS value of temperature fluctuation

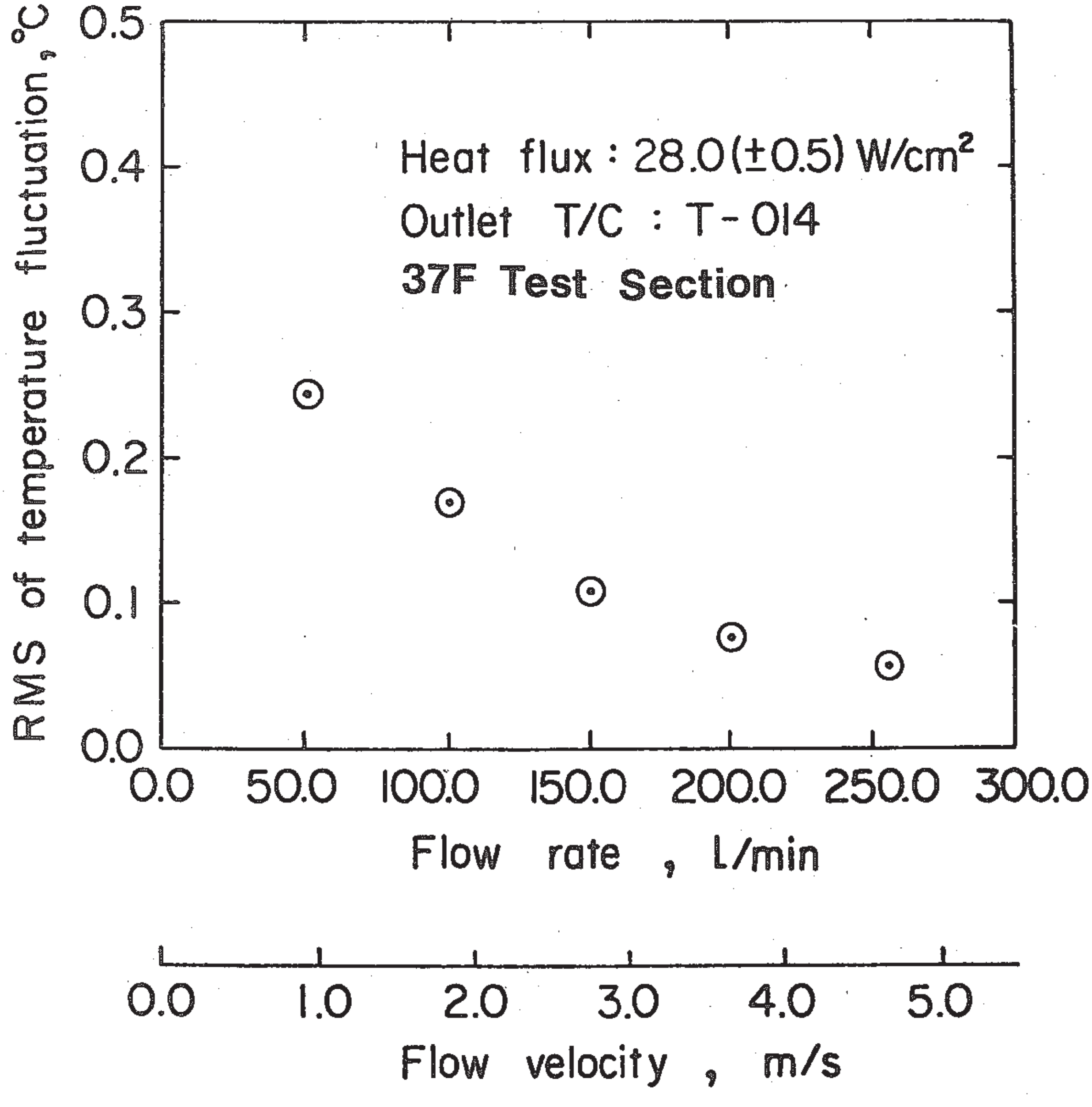

Fig. 3 (b) Effect of flow rate on RMS value of temperature fluctuation

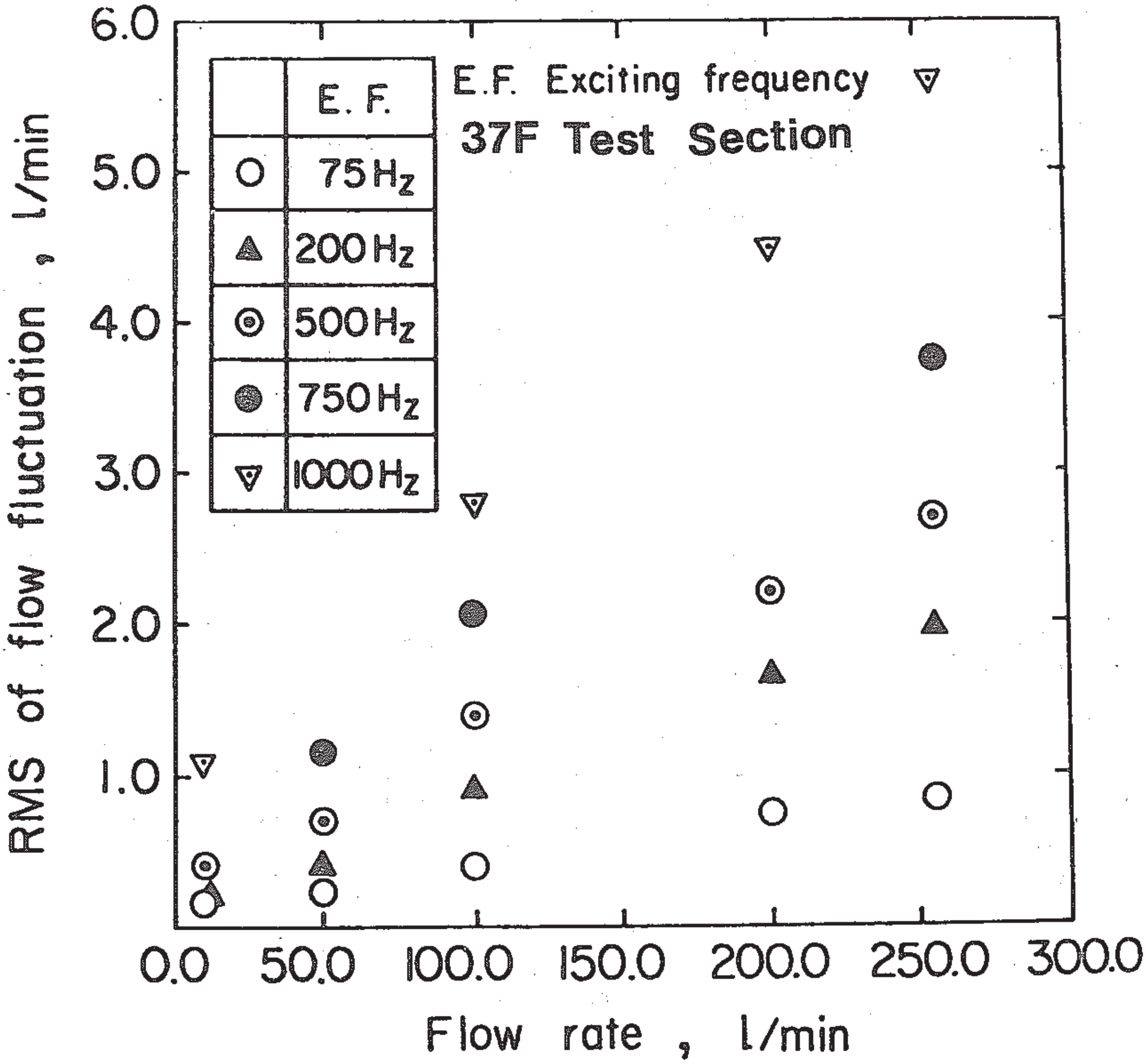

Fig. 3(c) Effect of flow rate on RMS value of flow fluctuation without gas release

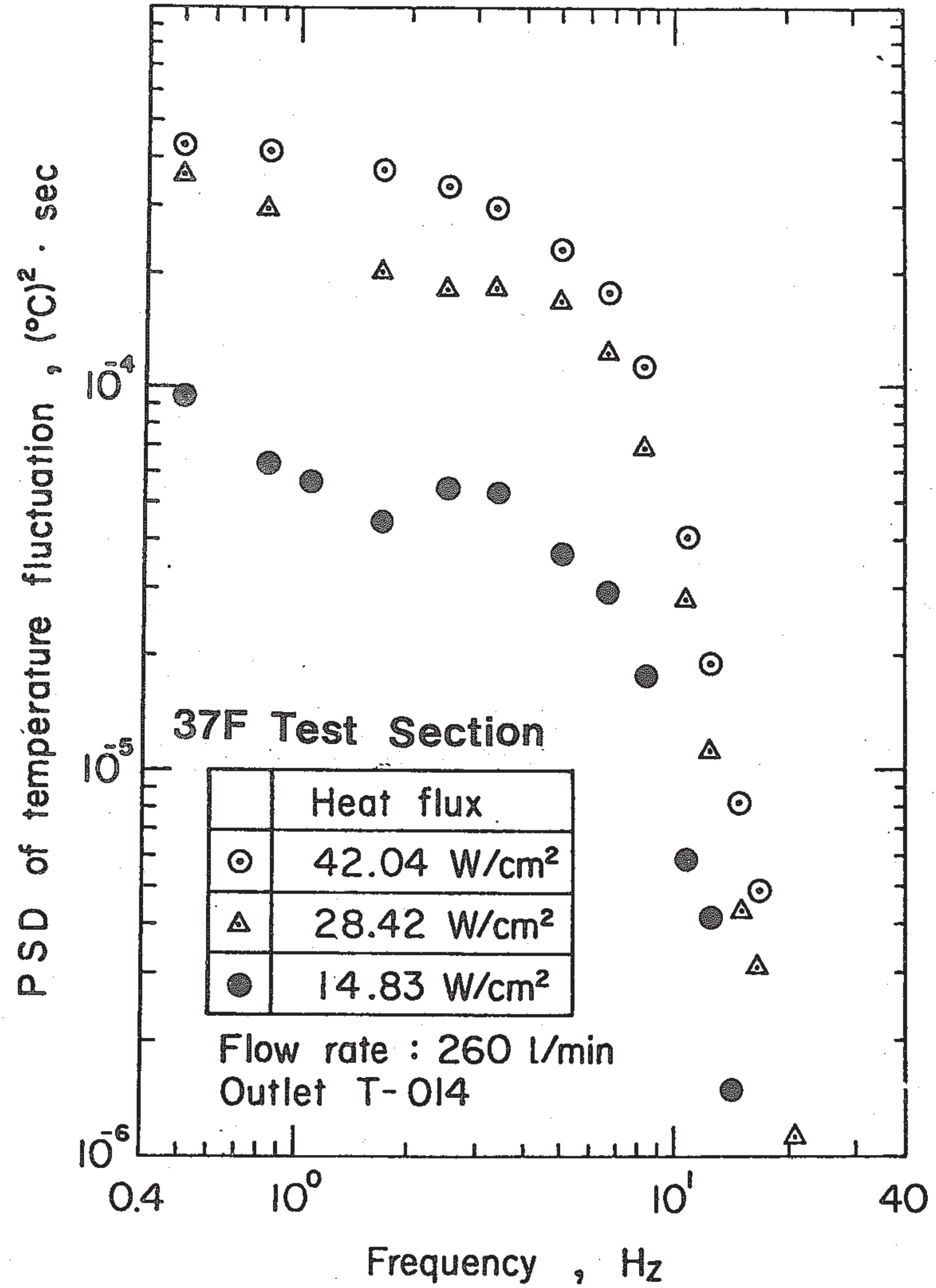

Fig. 4 (a) Effect of heat flux on power spectral density of temperature fluctuation

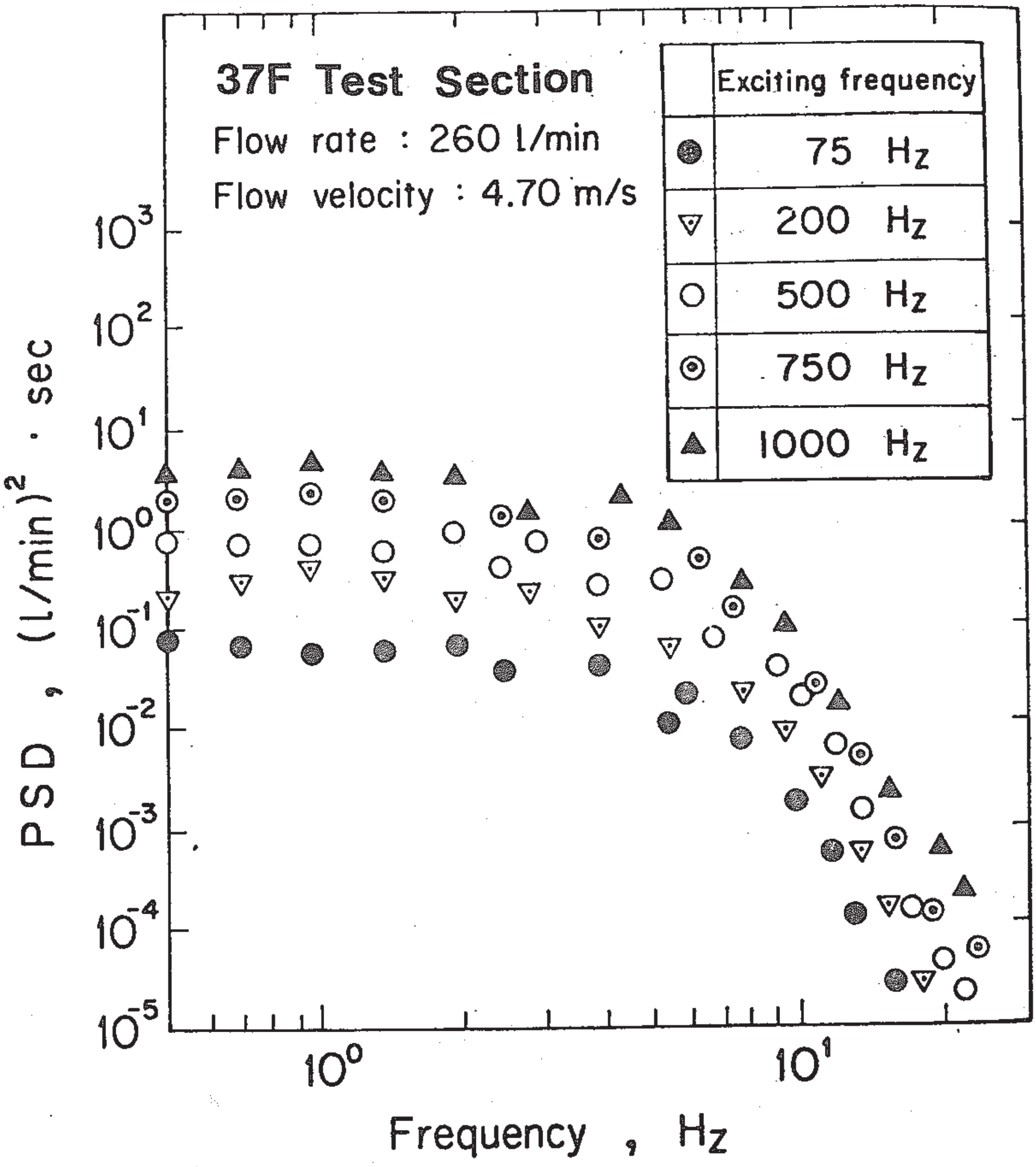

Fig. 4 (b) Effect of exciting frequency of eddy current type flow meter on PSD of flow fluctuation without gas release

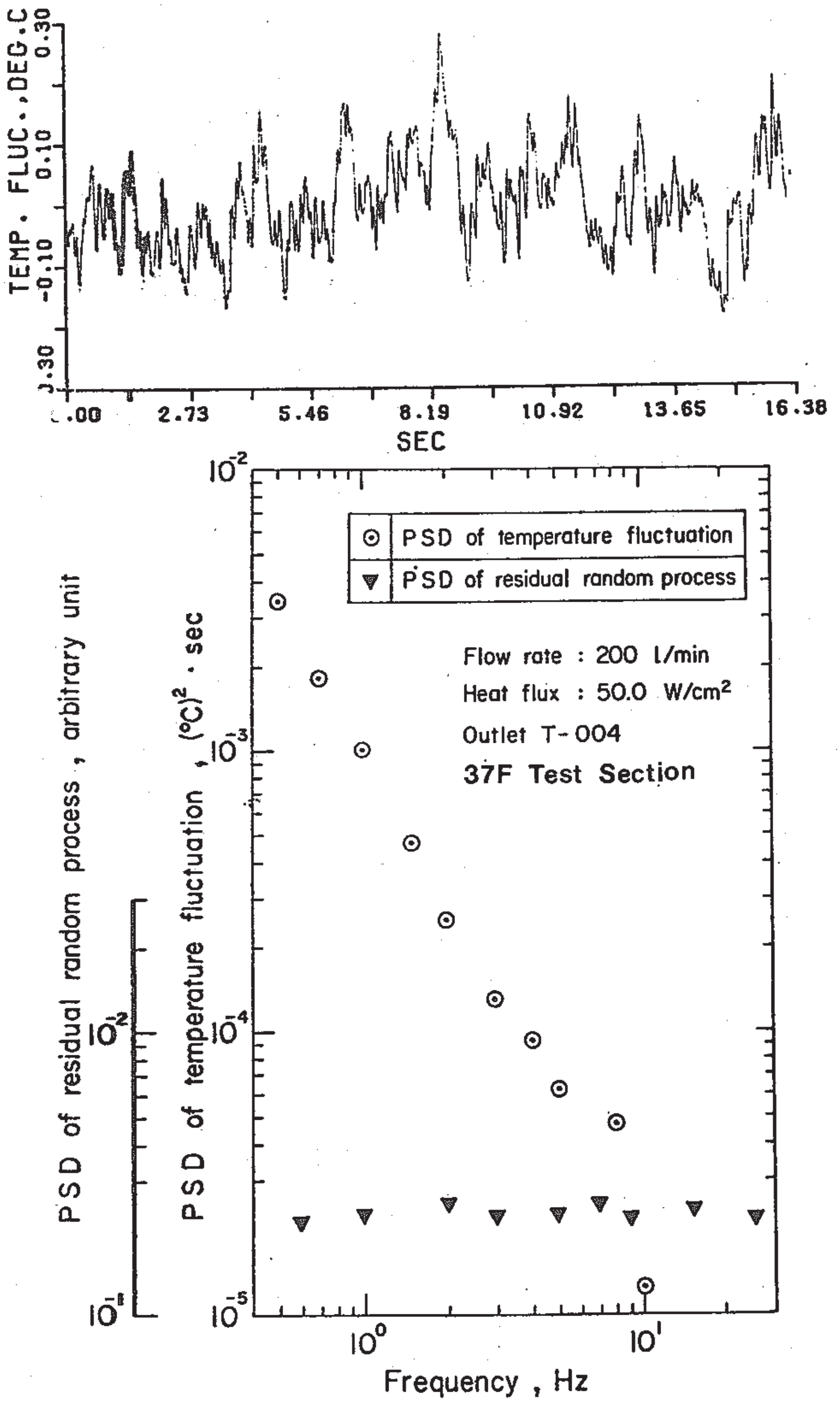

Fig.**5(a)** Power spectral densities of temperature fluctuation and its residual random process

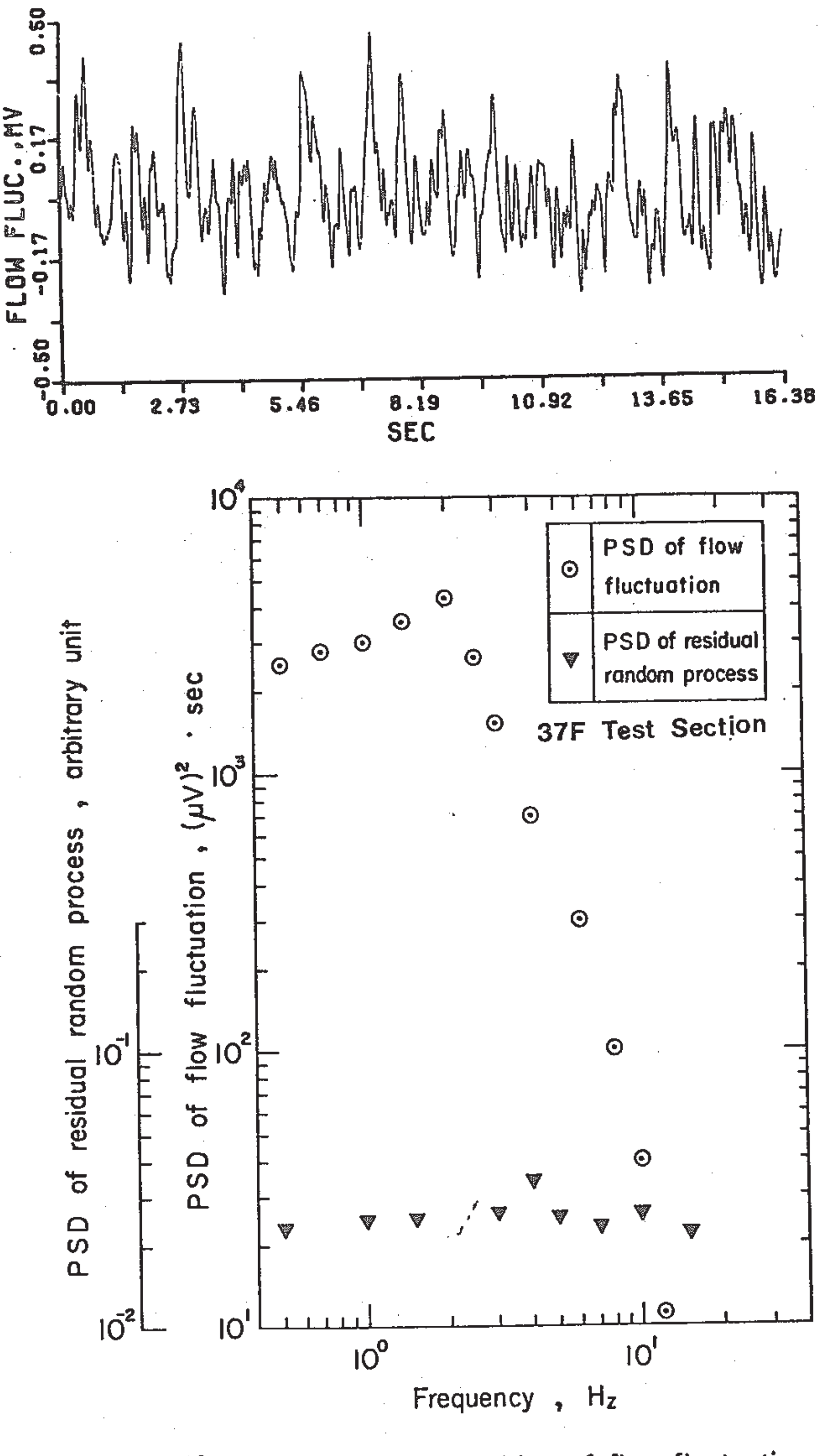

Fig. 5 (b) Power spectral densities of flow fluctuation and its residual random process

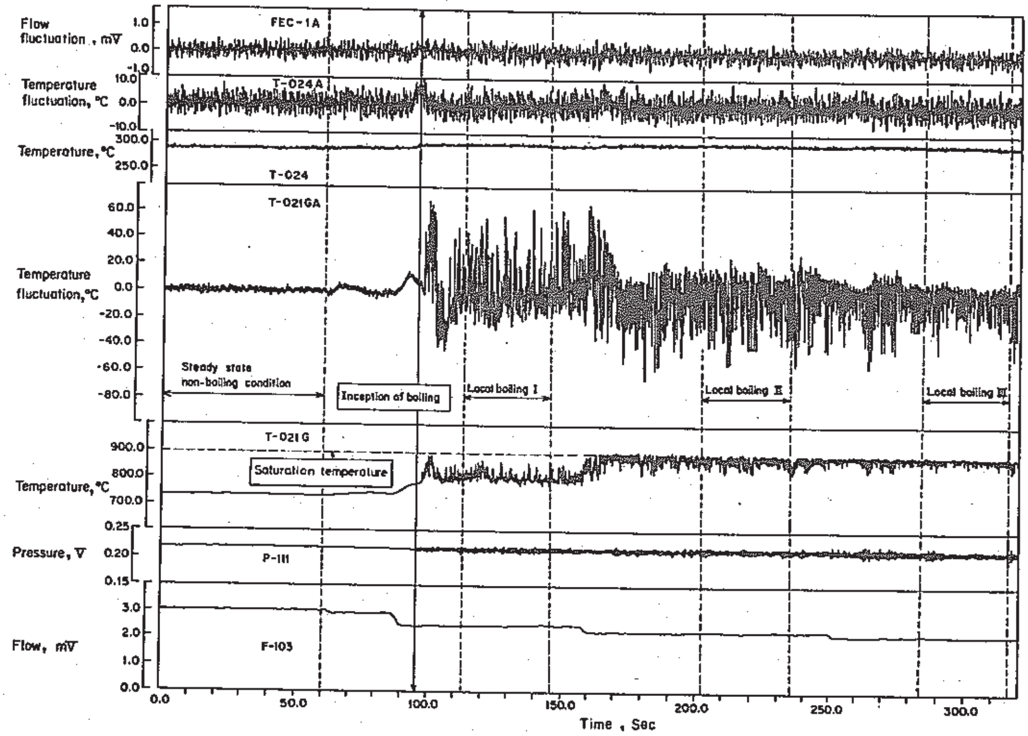

Fig. 6　Signals under local boiling condition (Run No. 61WLB-101)

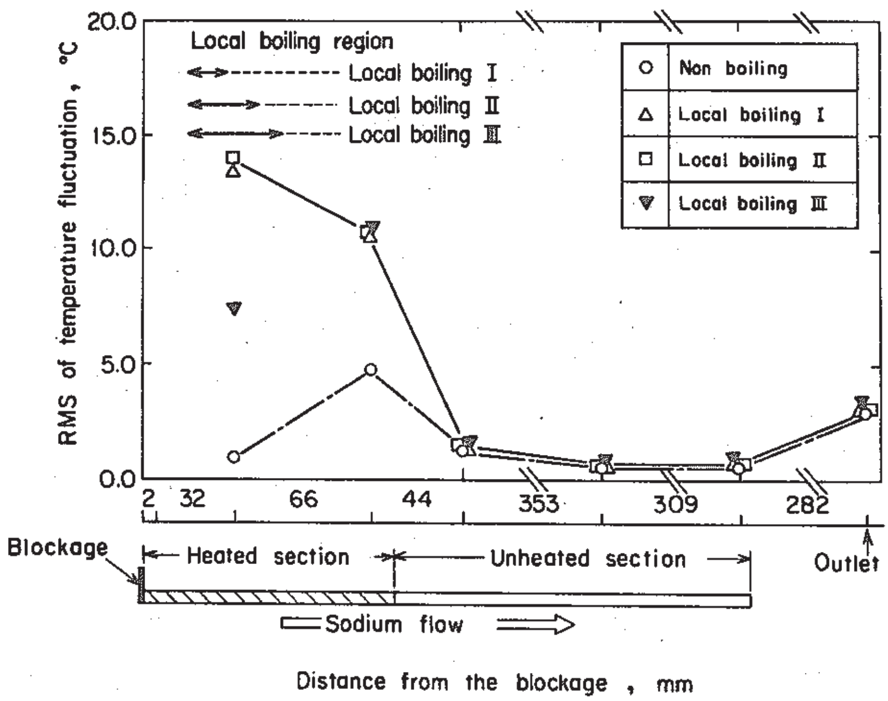

Fig. 7　RMS values of temperature fluctuations observed at several axial positions behind the blockage (Run No. 61WLB-101)

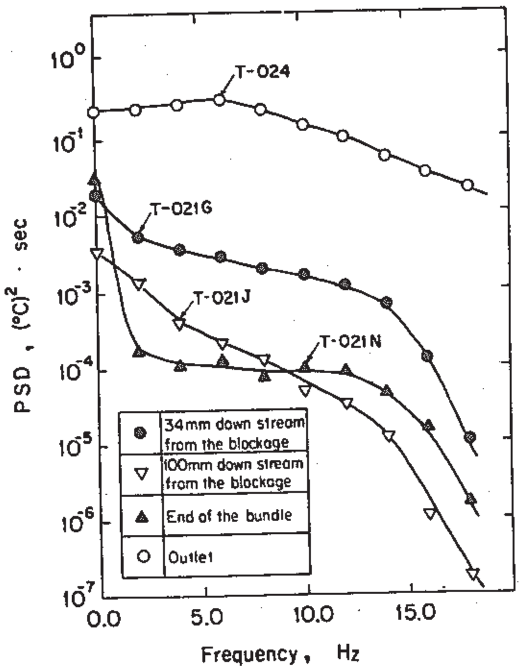

Fig. 8 Power spectral densities of temperature fluctuations observed at several axial positions,
— Non-boiling condition
(Run No. 61WLB-101)

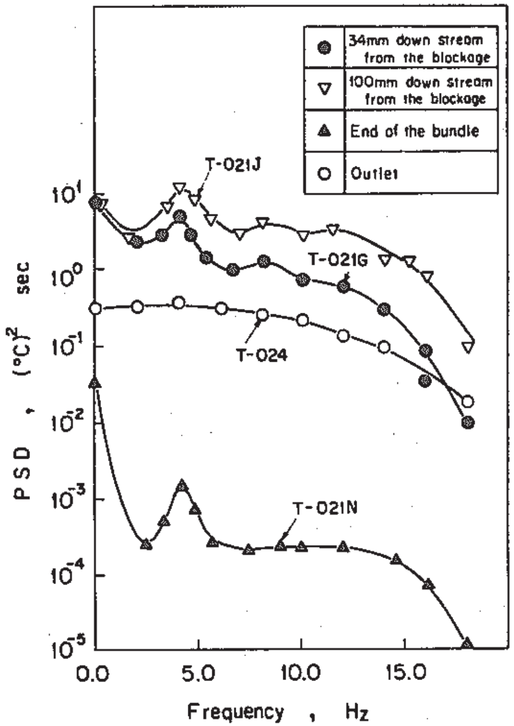

Fig. 9 Power spectral densities of temperature fluctuations observed at several axial positions,
— Local boiling III condition
(Run No. 61WLB-101)

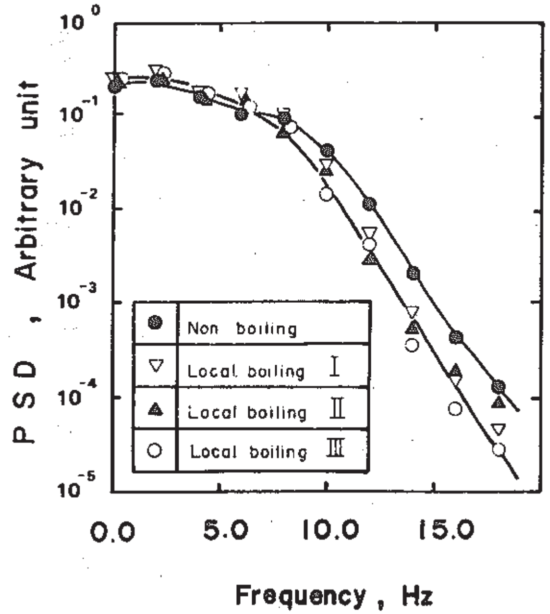

Fig. 10 Power spectral densities of flow fluctuation observed at the outlet of the bundle
(Run No. 61WLB-101)

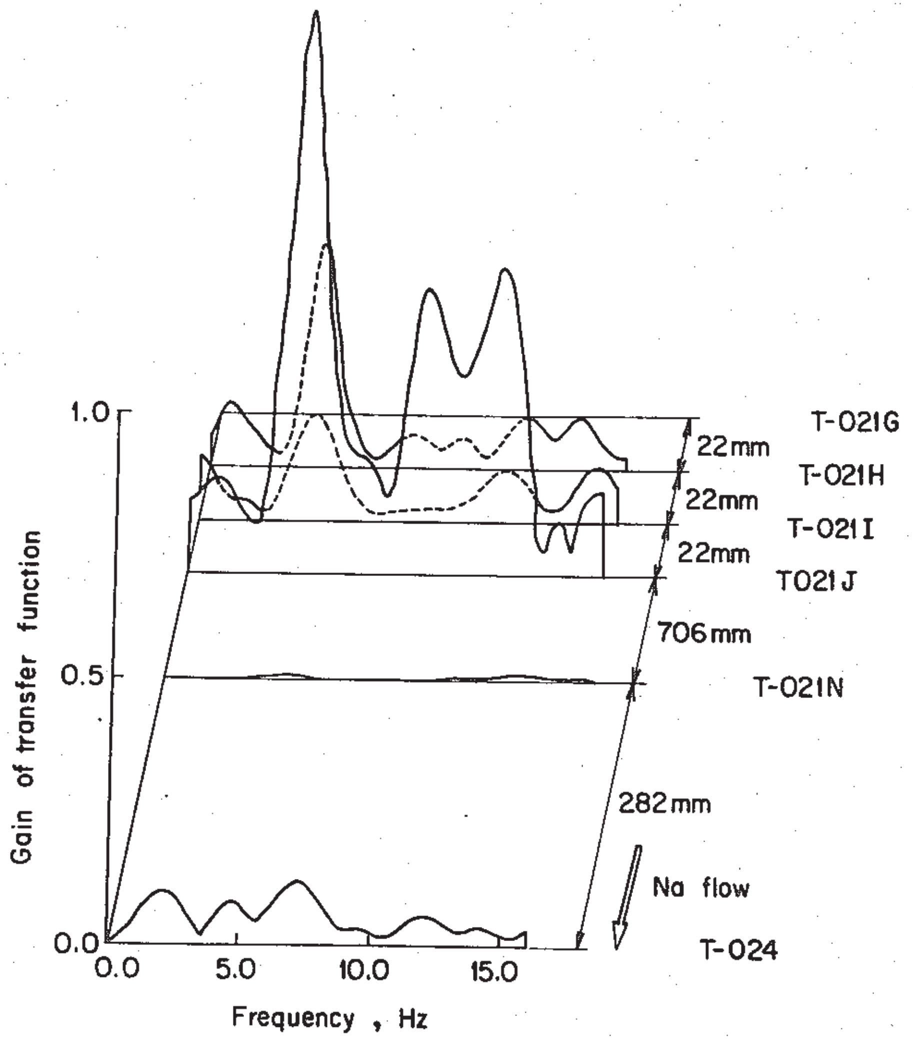

Fig. 11 Transfer functions between several couples of temperature fluctuations, one is T-021G and the opposite is one of the others (T-021H,..., T-024), -- Local boiling III condition (Run No. 61WLB-101)

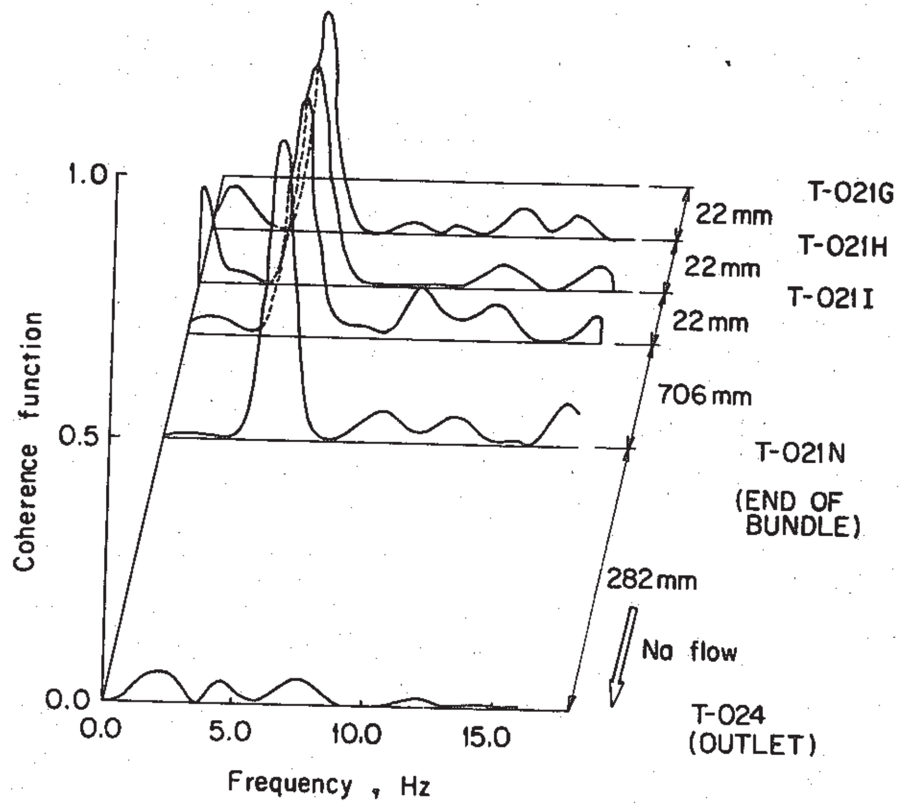

Fig. 12 Coherence functions between several couples of temperature fluctuations, one is T-021G and the opposite is one of the others (T-021H,..., T-024), -- Local boiling III condition (Run No. 61WLB-101)

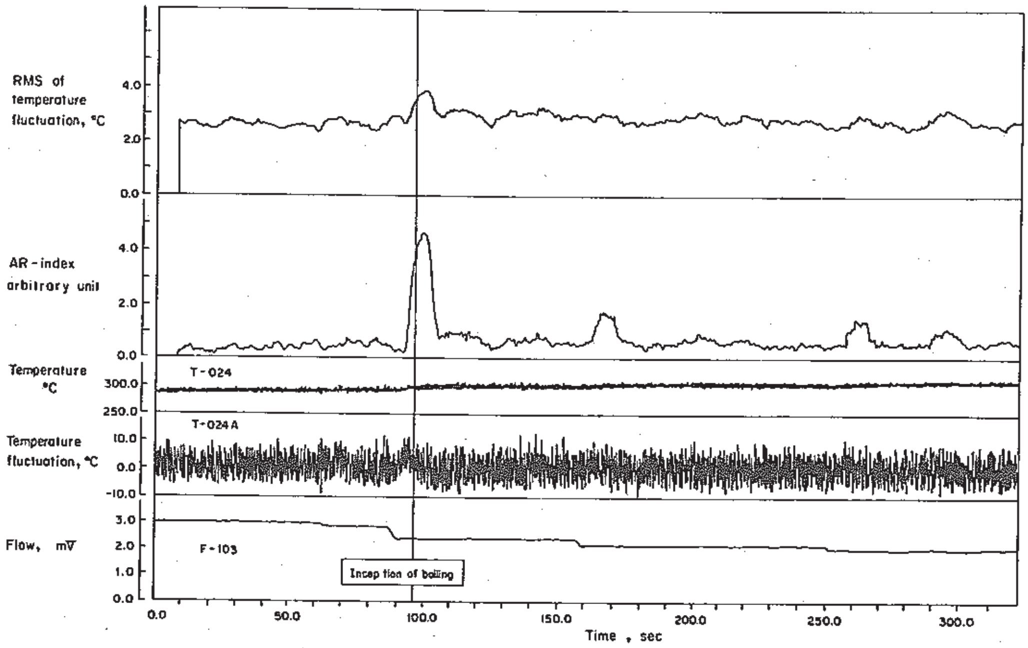

Fig. **13** RMS value and AR index of temperature fluctuation measured at the outlet of the bundle (T-024) (Run No. 61WLB-101)

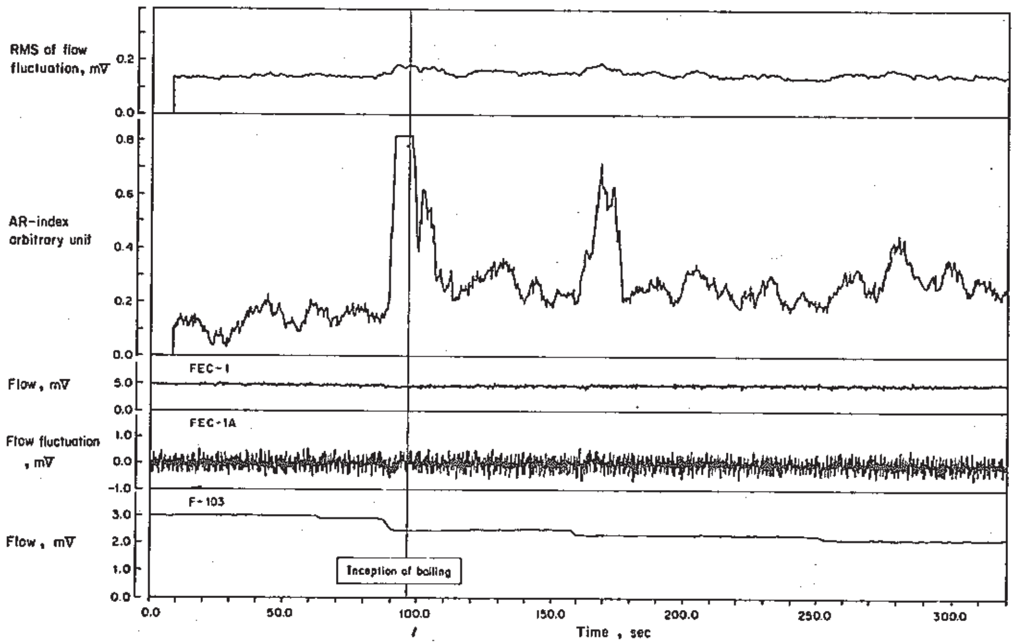

Fig. **14** RMS value and AR index of flow fluctuation measured at the outlet of the bundle (FEC-1) (Run No. 61WLB-101)

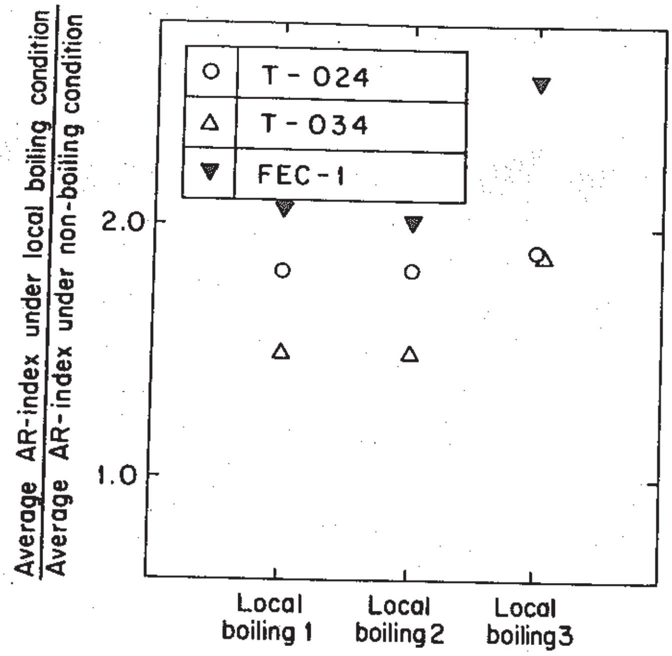

Fig. 15 Ratio of the average AR index under boiling condition to that under non-boiling condition (Run No. 61WLB-101)

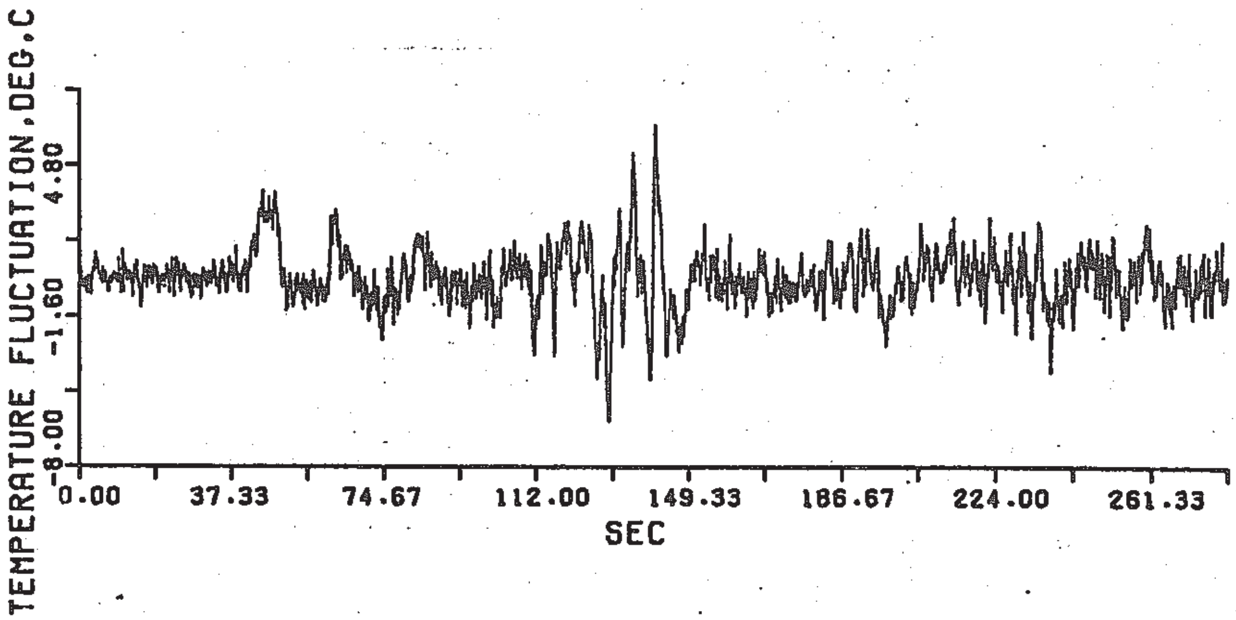

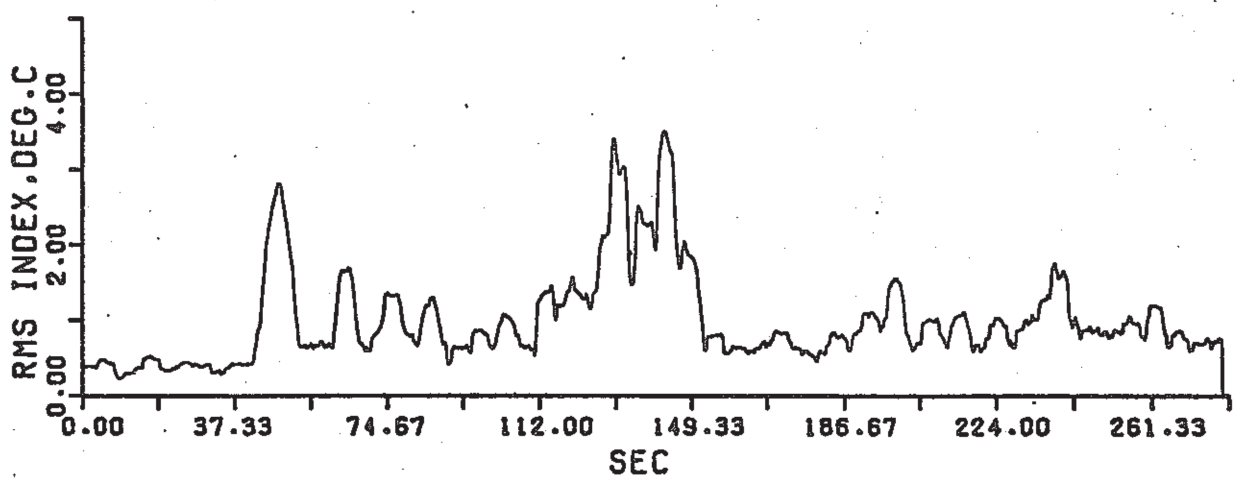

Fig.16 (a) Effect of thermocouple time constant on the local boiling detection: Time constant = 0.53 sec (Run No. 37(12)LB-129)

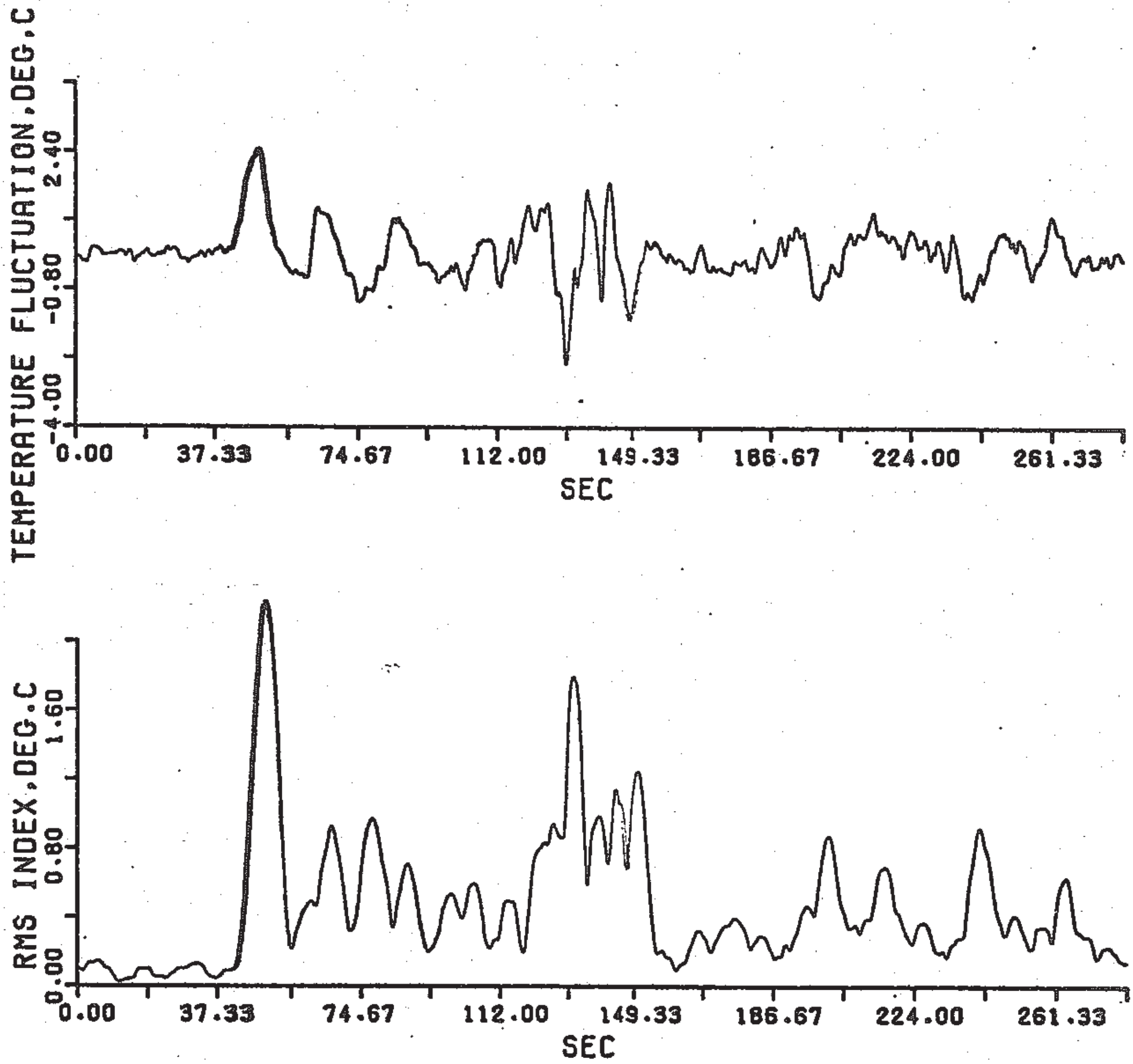

Fig.16 (b) Effect of thermocouple time constant on the local boiling detection: Time constant = 3.0 sec (Run No. 37(12)LB-129)

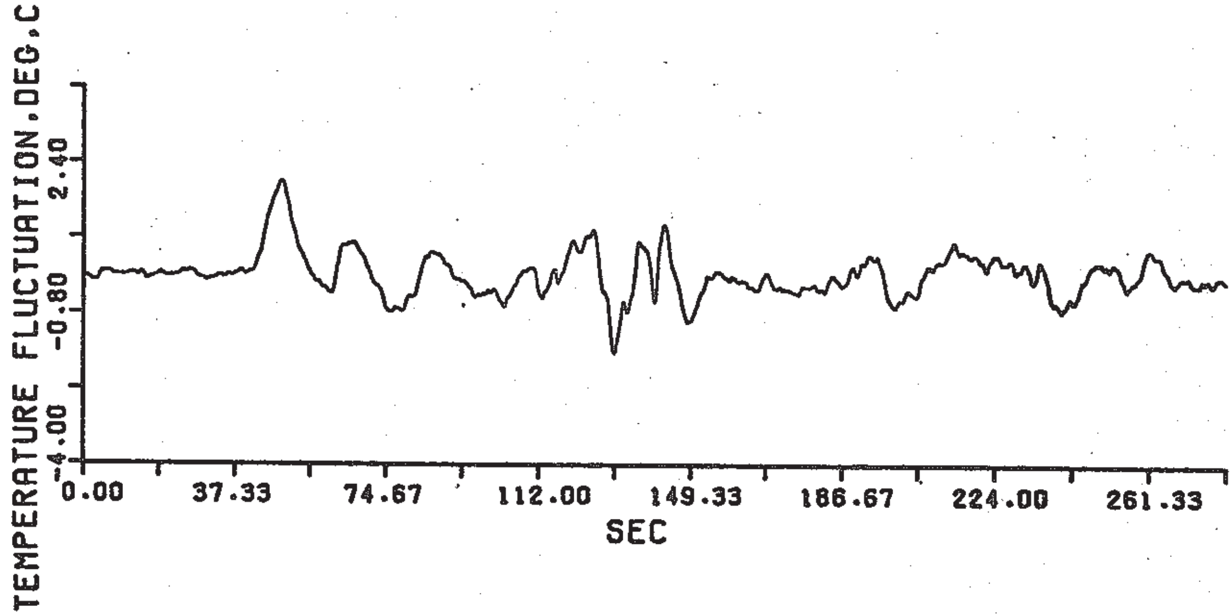

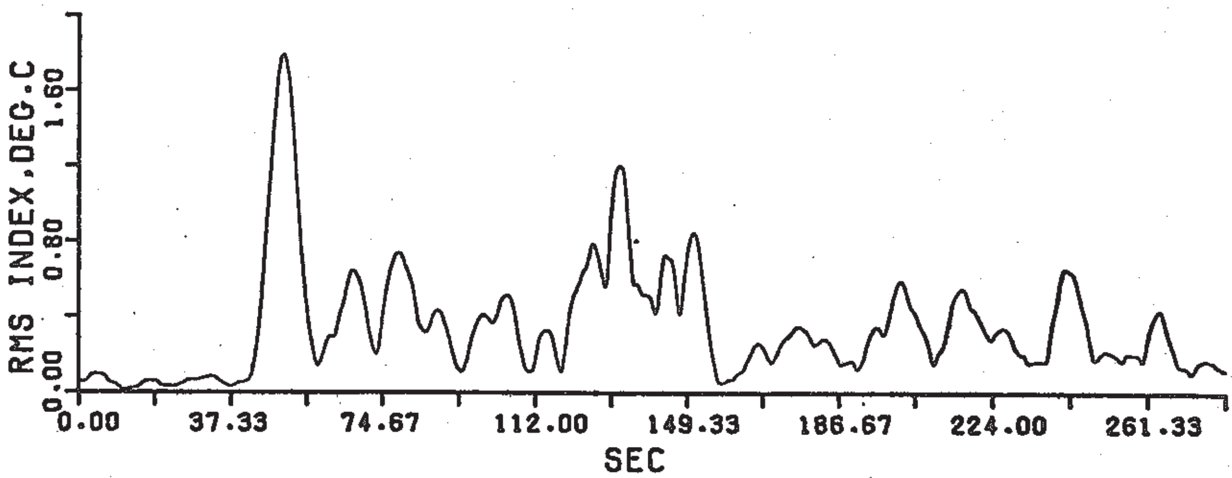

Fig. 16 (c) Effect of thermocouple time constant on the local boiling detection: Time constant = 5.0 sec (Run No. 37(12)LB-129)

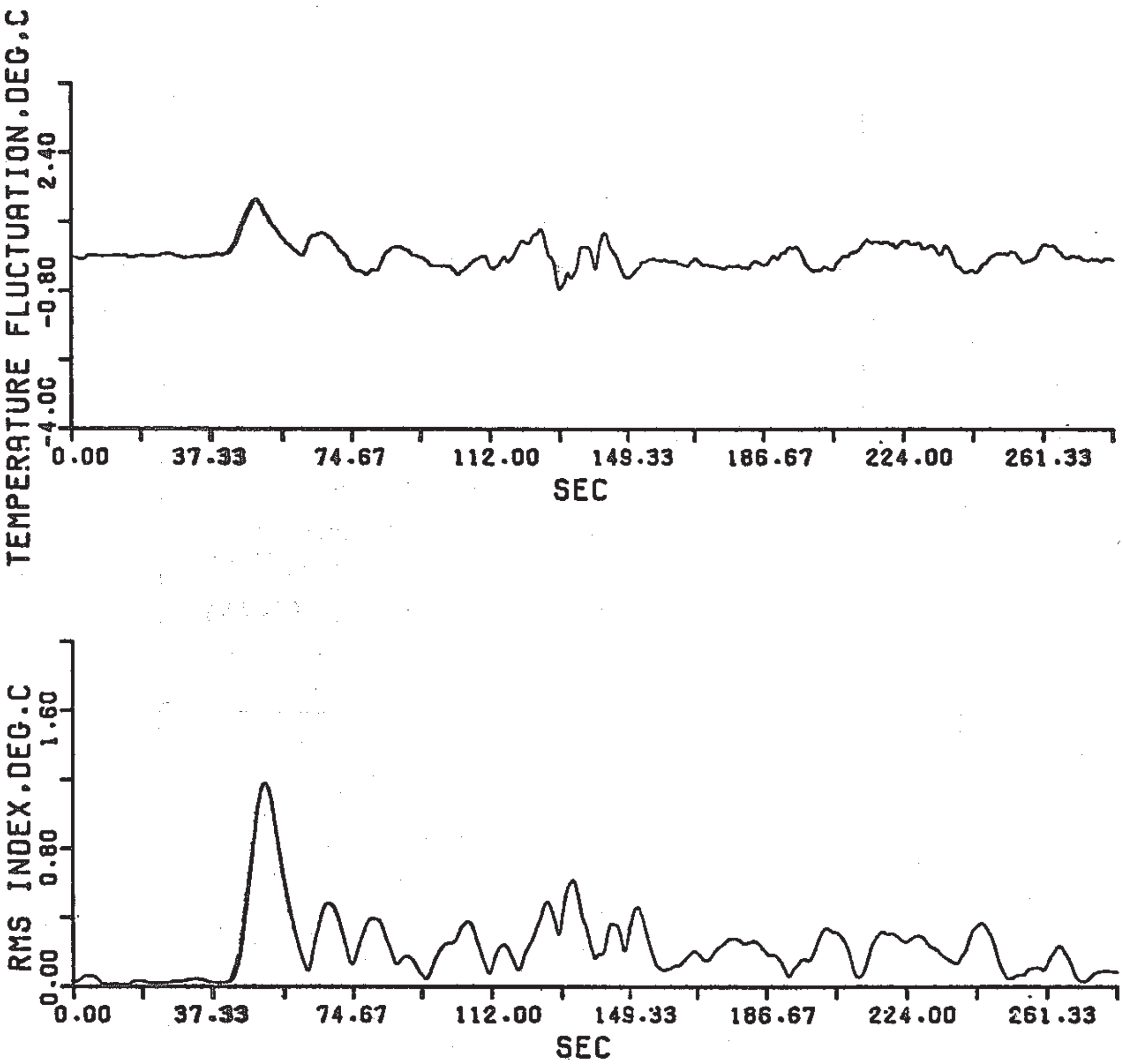

Fig. 16 (d) Effect of thermocouple time constant on the local boiling detection: Time constant = 10.0 sec (Run No. 37(12)LB-129)

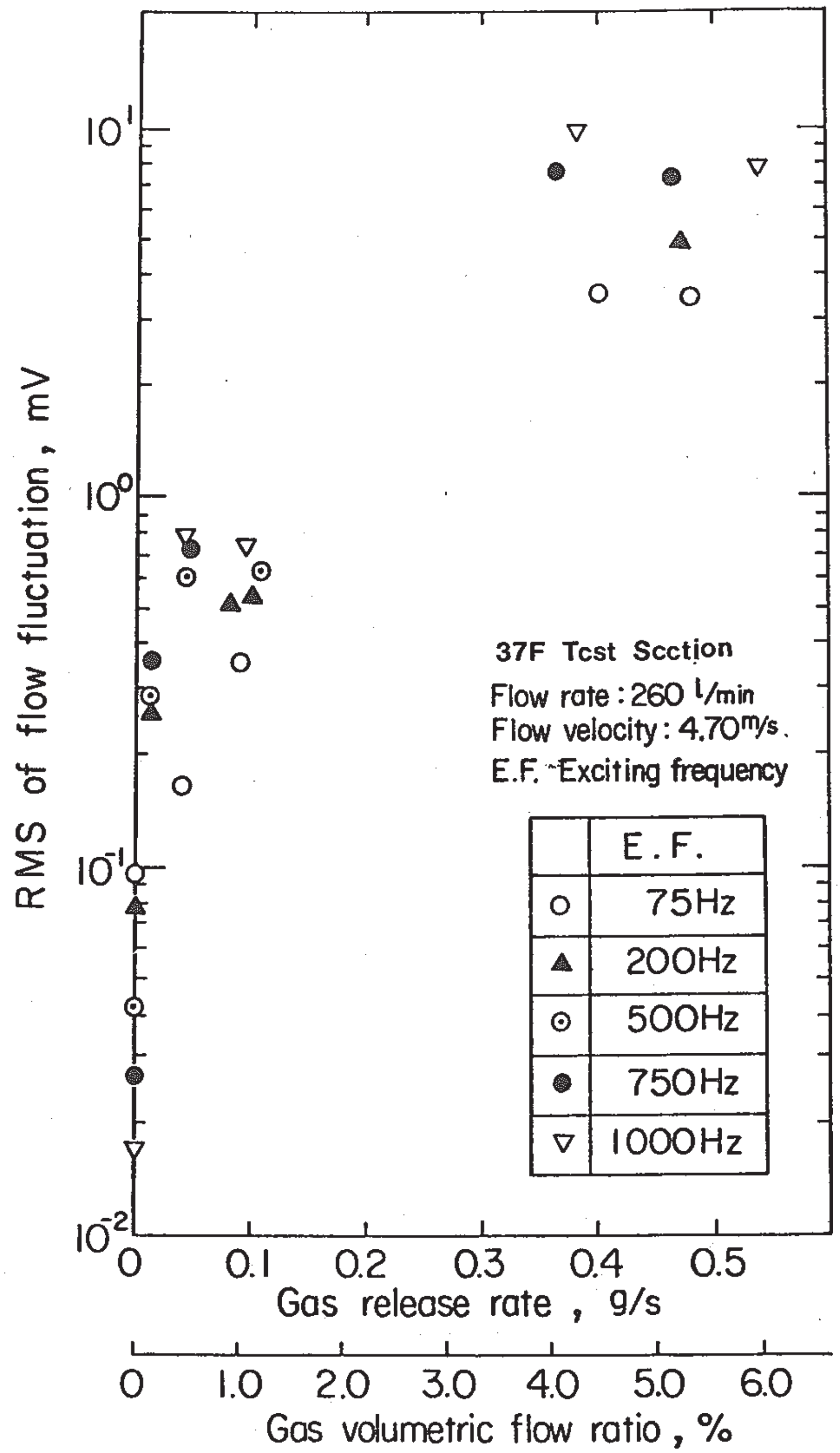

Fig. 17 Effect of gas release rate on RMS value of flow fluctuation

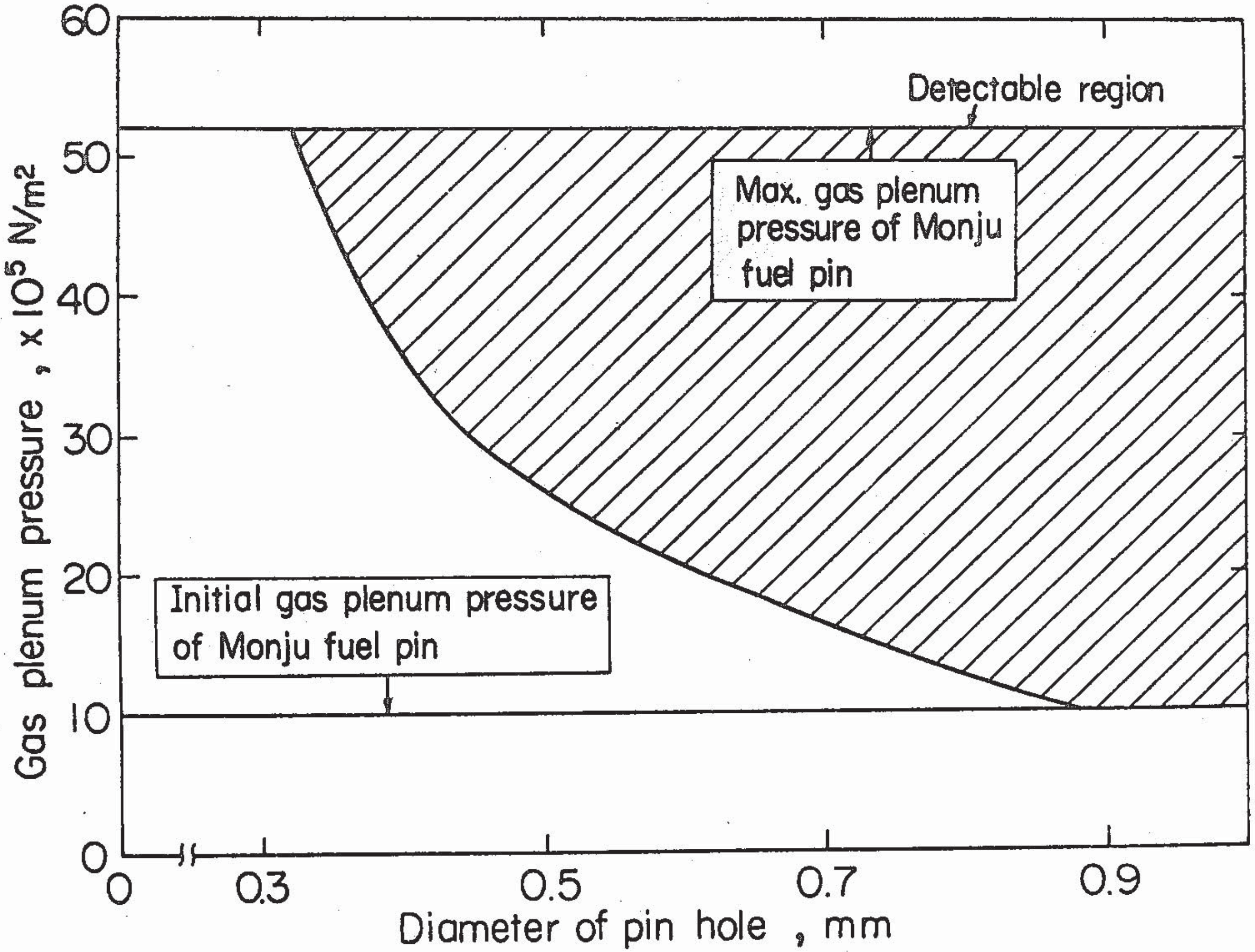

Fig. 18 Detectable conditions for cladding failure by use of eddy current type flow meter : exciting frequency 200Hz

(PNC-FS-1414)

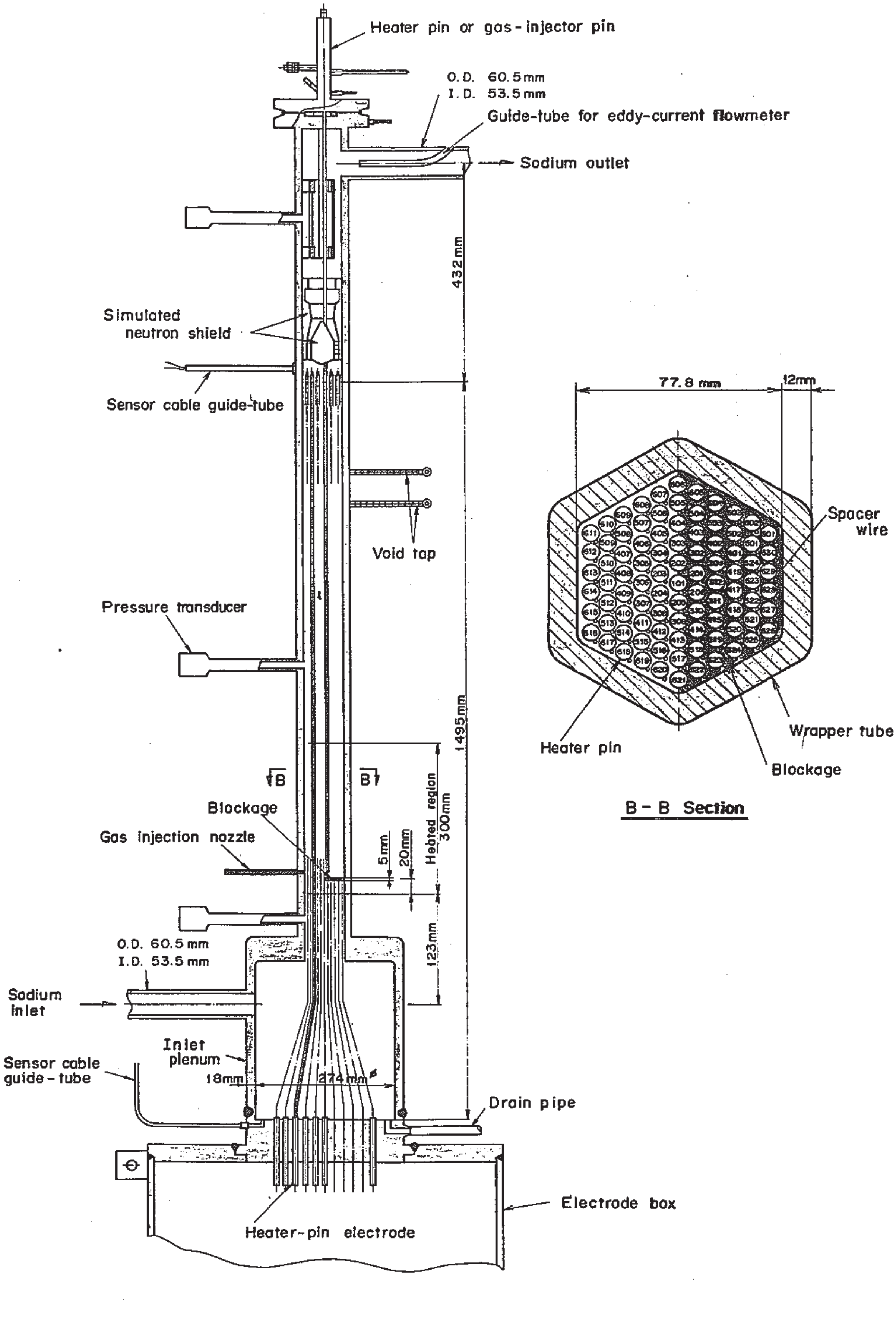

Fig. 19 Local blockage 91-pin bundle test section